Tractography with Physiology Rendering of Human Brain using Diffusion Basis Spectrum Imaging

Yong Wang[1], Peng Sun[1], Fang-Chang Yeh[2], Robert Naismith[3,4], Anne H Cross[3,4], and Sheng-Kwei Song[1,4]

[1]*Radiology, Washington University in St. Louis, Saint Louis, MO, United States,* [2]*Departments of Biomedical Engineering, Carnegie Mellon University, Pittsburgh, PA, United States,* [3]*Neurology, Washington University in St. Louis, Saint Louis, MO, United States,* [4]*Hope Center of Neurological disorders, Washington University in St. Louis, Saint Louis, MO, United States*

Introduction Diffusion tensor imaging (DTI) has been successfully applied to detect central nervous system (CNS) tissue injury [1]. To facilitate CNS injury detection using tract-based analysis, DTI-derived pathology-specific biomarkers can be rendered and projected onto white matter tracts generated by tractography [2]. However, DTI is not capable of modeling crossing fibers and subvoxel partial volume effect (resulting from inflammation, CSF contamination, or tissue loss) reduced the sensitivity and specificity of DTI biomarkers and the accuracy of tractography. Advanced diffusion MRI approaches have been developed to improve the tractography accuracy by improving the resolution of crossing fibers [CHARMED, DSI, HARDI, etc]. Unfortunately, none has taken into account of the inflammation associated cellularity and edema surrounding the white matter tracts. To fully address the limitation of current DTI and diffusion tractography, diffusion basis spectrum imaging (DBSI), was recently proposed and validated by both phantom and in vivo animal studies demonstrating its capability of resolving crossing fibers while still obtaining directional diffusivity as well as estimating the extent of inflammation [3]. In this study, we report the preliminary application of DBSI to the normal human brain in conjunction of the non-model base generalized q-sampling imaging (GQI) [4] to demonstrate DBSI utilities in human brains.

Method *Subject:* Eight normal healthy controls signed informed consent approved by the Washington University Institutional Review Board. *MRI:* A 3.0 Tesla Trio TIM (Siemens, Erlangen, Germany) scanner was used to acquire diffusion data. Both DBSI and GQI data were acquired with the 2.5x2.5x2.5 mm^3 resolution in the transverse plane, using single-shot diffusion-weighted EPI. GQI data were acquired using 256 grid sampling points with the maximum b-value = 4000 s/mm^2 [5], resulting in a scanning time of 36 minutes. DBSI data were acquired using 99 diffusion weighting also on grids with maximum b-value = 2200 s/mm^2, resulting in a scanning time of 12 minutes. *DBSI Analysis:* Eq. [1] was solved by fitting the 99 diffusion weighted signals using a linear combination of diffusion basis sets to estimate the number of anisotropic diffusion tensor components (N_{aniso}) and the associated principal directions [3]. After N_{Aniso} was computed, the number of isotropic component (N_{iso}) was further determined using nonnegative least-squares analysis. The global nonlinear optimization was conducted employing direct pattern search to solve Eq. (1). S_k is the k^{th} measured diffusion weighted signals. S_i and S_j are fractions of anisotropic diffusion components and isotropic diffusion component respectively [3]. *GQI Analysis:* All diffusion weighted dataset were reconstructed using GQI with a diffusion sampling ratio of 1.25, the recommended parameter proposed by the original study [4]. *DBSI Fiber Tractography:* Modified whole brain streamline fiber tracking [6] was conducted using the fiber orientations derived by DBSI. The maximum turning angle was 60°. DBSI-derived fiber ratio was used as the termination parameter. The tractography and rendering are conducted using DSI Studio [7].

$$S_k = \sum_{i=1}^{N_{Aniso}} S_i e^{-\left|\vec{b}_k\right|\lambda_\perp} e^{-\left|\vec{b}_k\right|\left(\lambda_\parallel-\lambda_\perp\right)\cos^2\theta_i} + \sum_{j=1}^{N_{iso}} S_j e^{-\left|\vec{b}_k\right| d_j} \quad [1]$$

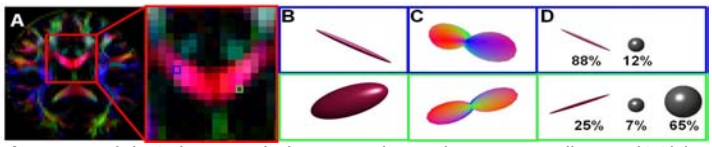

Figure 1 In (A), Color-encoded DTI FA shows the corpus callosum (CC) in red. DTI (B), GQI (C), and DBSI (D) results from 2 voxels in the CC (blue and green boxes) are presented in the form of diffusion ellipsoids (B, D) or 3D shell surfaces (C). DBSI-derived isotropic diffusion tensors are visualized by spheres with volume fractions given. Although all methods correctly detected fiber orientation, only DBSI correctly quantified diffusivities and volume ratios of each component.

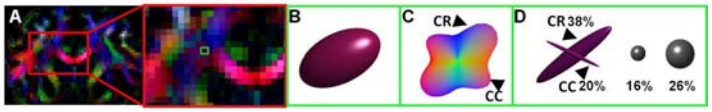

Figure 2 Similar to Fig.1, for the green voxel where corpus callosum crosses corona radiata (A), DTI failed to detect fiber crossing (B). Although GQI (C) and DBSI (D) correctly detected crossing fibers, only DBSI was capable to quantify directional diffusivities for each fiber as well as the subvoxel ratios of fiber tracts, cellularity and extra-cellular space.

Results and Discussion Two voxels within the normal corpus callosum were analyzed (Fig. 1). One located entirely in the corpus callosum (CC) and the other was located partly in the ventricle. Although DTI correctly determined the fiber orientation for both voxels, DTI-derived axial and radial diffusivities for the second voxel were much larger than those for the first voxel (Axial diffusivity 1.71 vs. 1.45 $\mu m^2/ms$; Radial diffusivity 0.7 vs. 0.1 $\mu m^2/ms$), due to the partial volume effect of ventricular CSF. GQI correctly reflected the fiber orientations, but unable to quantify the fiber's directional diffusivities. In contrast, DBSI correctly determined the fiber orientation in the two voxels while quantified the extent of CSF partial volume effect in the second voxel. After removing the confounding isotropic components due to cells (12% and 7% for the first and second voxel) and extracellular space, i.e., CSF contamination, (0% and 65% for the first and second voxel), DBSI-derived axial and radial diffusivity was consistently determined for both voxels (Axial diffusivity 2.25 vs. 2.30 $\mu m^2/ms$; Radial diffusivity 0.11 vs. 0.12 $\mu m^2/ms$). Another representative voxel where CC crosses with corona radiata (CR) was analyzed (Fig. 2). DTI did not detect the fiber crossing at all. Both GQI and DBSI correctly resolved the orientations of CC and CR. In addition, DBSI quantified the volume ratios of CC (20%) and CR (38%). The directional diffusivities for the CR were: axial diffusivity = 1.93 $\mu m^2/ms$ and radial diffusivity = 0.25 $\mu m^2/ms$, and for CC were axial diffusivity = 2.09 $\mu m^2/ms$ and radial diffusivity = 0.10 $\mu m^2/ms$, which were in close agreement with the results obtained for CC without crossing fibers (Fig. 1). The above voxel-based analysis provided solid basis for whole brain DBSI computation. DBSI-based whole brain tractography generated accurate connection information of white matter tracts (Fig.3 A, C). DBSI-derived various diffusion indices can be further rendered onto this tractography to provide tract-based pathophysiology information. For example, fiber ratio based rendering (Fig.3 B, D) demonstrated that the central region (horizontal arrows) of CC had the highest fiber density, whereas the superior edge (downward arrows) had a lower fiber ratio due to the contamination of gray matter. The inferior edge (upward arrows) also has lower fiber ratio because of the contribution of CSF of ventricle. This pilot study provided base for the future clinical translation of DBSI to various CNS disorders.

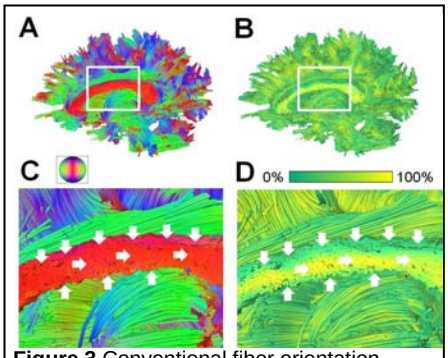

Figure 3 Conventional fiber orientation rendered tracts only provides connection information of white matter tracts (A, C), while DBSI fiber ratio rendered fiber tracts (B, D) could reveal fiber density along fiber tracts.

References: [1] Song, SK. *et al*. *Neuroimage*. 2002; 17:1429. [2] Mori, S. *et al*. *NMR in Biomedicine*. 2002; 15:468-480. [3] Wang,Y. *et al*. *Brain*. 2011. 134: 3590; [4] Yeh, FC. *et al*. *IEEE Trans Med Imaging* 2010; 29; [5] Kuo, LW. *et al*. *Neuroimage*. 2008; 41. [6] Assaf,Y. *et al*. *Neuroimage*. 2005; 27: 48-58; [7] Yeh, FC. *et al*. *Neuroimage.*2011; 55, 1054-62.